



# Power Injection Model and Optimal Placement of an Electric Spring in a Distribution System

Mrutyunjaya Nanda\* and Jai Govind Singh\*.<sup>1</sup>

[www.ericjournal.ait.ac.th](http://www.ericjournal.ait.ac.th)

**Abstract** – The past decade has accelerated growth in using renewable energy sources for power generation. The intermittent nature of these sources, especially solar and wind, and their increased penetration in power systems threatened the grid's security by creating voltage fluctuations. Electric Spring is a recent novel concept that provides electric voltage support to the grid. The novelty of this study is developing a steady-state power injection model for the Electric Spring and incorporating it to optimally place the device in a distributed power system based on the voltage sensitivity index (VSI). This model also portrays the Electric Spring as a smart load when used with a dissipative electric load. The suggested model is independent of the bus voltages and branch currents; rather, it depends only on the parameters of the Electric Spring. The effectiveness of this suggested methodology is tested on 14-bus, 33-bus and 69-bus distribution networks. In each case, the node voltages and real and reactive powers injected at each bus are found to be better, and the performance of the ES with a DSTATCOM is also compared.

**Keywords** – Electric Spring, DSTATCOM, Power Injection Model of Electric Spring, Optimal Placement of ES.

## 1. INTRODUCTION

Conventional energy sources are limited in stock and even cause harm to the environment. Hence, countries are slowly but surely switching to renewable sources. The power generations from these sources are distributed in nature and involve several technical constraints at every stage. For example, issues like islanding, harmonic distortions and electromagnetic interference are pretty important [1]. However, one key physical aspect of sources like wind and PV, which are abundant, is their intermittent nature. According to ref. [2], the impact of intermittency can be either steady state or dynamic in nature, and they include, e.g., voltage fluctuation issues, changes in feeder voltage profiles, including voltage rise and unbalance, and reactive power flow fluctuations due to the operation of switched capacitor banks.

Many technologies have been adopted to mitigate the undesirable effects of voltage deviations. Synchronous Condensers are used as the grid's basic source of reactive power. Series and shunt capacitors are also optimally placed as reactive power sources. Apart from that, many FACTS devices are also used. They include STATCOM, SVC, TCSC and UPFC [3]. Each of these methods has its advantages and disadvantages. Synchronous Condensers contribute to the short-circuit current and are very expensive devices [3]. The problem with shunt capacitors is that they cannot be used in low voltages when needed the most and offer a slower response. To overcome the issues above, FACTS devices that are cheaper and smaller are currently the

preferred option. The popularity of these devices is due to the fact that they are all power electronics based and can be controlled conveniently [4].

In power systems, we come across various loads; certain loads need the voltage across them to be strictly regulated. Such loads have been termed as “critical” loads. The loads that can be operated with some degree of voltage fluctuation are termed “non-critical” loads. These include dissipative loads like water heaters, lighting systems and refrigerators [5]. So, voltage fluctuation becomes an issue when a critical load is placed in a grid with intermittent distributed generation sources embedded in it. Thus, to regulate the voltage across such critical loads, a smart device concept called the “Electric Spring (ES)” has been envisaged [6]. Once implemented, this innovative concept can stabilize the power systems with a significant penetration of renewable energy sources. Non-critical (NC) loads, when combined with ESs, give rise to a new set of loads called “smart loads”, which have their power demand following the power generation profile and not the other way around. Apart from voltage control, ES has a variety of other applications that include frequency fluctuation control [7]. The ref. [8] presented a new application of electric spring to ensure constant power across the loading elements under impedance variations. The ref. [9] proposed that the stable operation of rural power grids can be achieved by employing a photovoltaic-electric spring (PV-ES) device.

In addition, the imminent increase in intermittent and distributed renewable power sources has raised concerns about the stability of the power grid. Voltage fluctuations are one of the most common effects of grid integration of renewables. The ES, a novel smart device concept, can replace the commonly used reactive power compensators to mitigate these problems. However, most of the existing literature focuses on the ES concept, load characterizations and its control [6], [10]. In ref.

\*Department of Energy, Environment and Climate Change, SERD, Asian Institute of Technology, Klong Luang, Pathumthani-12120, Thailand.

<sup>1</sup> Corresponding author;  
E-mail: [mrutyunjaya.n@asiacleanenergypartners.com](mailto:mrutyunjaya.n@asiacleanenergypartners.com);  
[jgsingh@ait.ac.th](mailto:jgsingh@ait.ac.th).

[11], the application of DC electric springs in DC distribution networks is studied. DC electric springs are introduced to the non-critical load side, which can enhance the flexibility of loads. Reference [12] work proposed a multi-objective voltage control for multiple Electric Springs (ESs) in active unbalanced distribution systems. The effect of connecting an ES on the various network parameters has not yet been explored. Further, unlike other FACTS devices, a steady-state analysis of the power consumed and supplied by the ES when it is connected to a network is yet to be conducted. Therefore, the behavior of the grid when an ES is connected has been studied very little.

This paper suggests a new static Power Injection Model of ES for power flow and static voltage stability analysis. The same model is then used to evaluate the effect of placing an ES in a distribution network by running load flows with and without an ES. At the same time, the candidate bus for the optimal placement of an ES in a radial distribution network is found, considering the system's Voltage Sensitivity Index (VSI). The effectiveness of the suggested methodology of ES application is compared with DSTATCOM. However, it is worth mentioning that here, the ES being conceived will be able to handle voltage fluctuations of a few volts and not huge swings.

## 2. MODELING OF TOOLS AND EQUIPMENT

In 1678, Robert Hooke, for the first time, explained the working of a mechanical spring (Hooke, 1678) [6], [10]. It is a device that basically has the following three functions: i) provide mechanical support, ii) store mechanical energy, and iii) damp mechanical oscillations [13]. It stores energy in the form of potential energy. When the spring is compressed or stretched, it is displaced by an amount proportional to the force applied. The applications of mechanical springs in our daily lives are widespread. Generally, they are used in the form of an array, where they collectively support a mattress or a vehicle seat. Even though spring fails, the rest can support the mattress in this arrangement. An ES uses this simple concept in the power grid to maintain a constant voltage across the critical load.

Analogous to a mechanical spring, an ES also has three basic functions: i) provide voltage support, ii) store electrical energy, and iii) damp electric oscillations. Thus, the expressions that are similar to Equations (1) and (2) are as follows,

$$q = \begin{cases} CV \\ -CV \end{cases} \quad (1)$$

$$PE = \frac{1}{2} CV^2 \quad (2)$$

where,  $v_a$  is the voltage across the capacitor and it can be controlled by controlling the charge  $q$  through it. The current  $i_c$  in turn, it controls the charge, which Equation (2) gives. Hence, the ES can be referred to as a “current-controlled voltage source.”

### A. Operating Principles of an Electric Spring (ES)

An ES is an ingenious device that can be installed in series with NC load(s), like a central air-conditioning system, which can bear voltage fluctuation in a renewable energy-based micro-grid as illustrated in Fig. 1 [14]. This series connection maintains voltage at device installation  $V_s$  to the reference value  $V_{s-ref}$ . As shown in Fig. 1, the critical load is attached in parallel to the smart load comprising of ES and NC load, and the voltage across it is  $V_s$ . Also, ES can be utilized for both active and reactive power compensation [9]. For an ES to be lossless, the compensation voltage vector  $V_a$  has to be perpendicular to the NC load current  $I_o$  (Fig. 2). This means for a resistive-inductive load,  $V_a$  should be leading  $I_o$  by  $90^\circ$  and gives capacitive compensation and vice-versa for an inductive compensation.

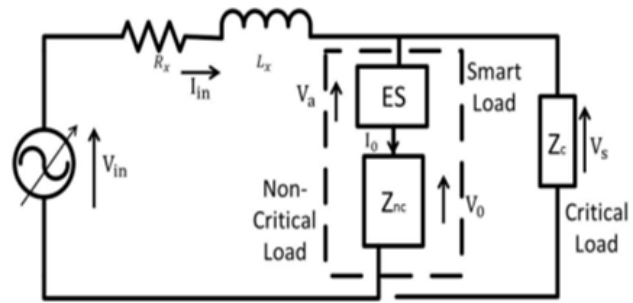


Fig. 1. Overview of ES in series with a non-critical load [14].

It is illustrated through vector diagrams in Fig. 2 [14]. The phasor sums of the NC load voltage  $V_o$  and the compensation voltage  $V_a$  equals the voltage at device installation  $V_s$ . In steady-state conditions, vector Equation (3) for voltage can be written as:

$$V_s = V_o + V_a \quad (3)$$

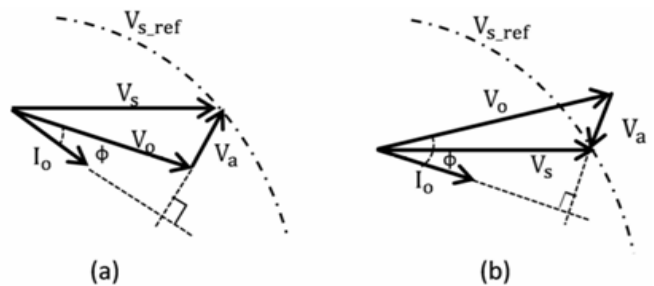


Fig. 2. Phasor Diagrams of ES circuit parameters with a resistive-inductive load in (a) capacitive mode (b) inductive mode.

When the rms voltage across the critical load  $V_s$  is less than the reference rms voltage  $V_{s-ref}$  (230 V), the ES boosts it up instantaneously to the reference value, by adjusting the voltage across the non-critical load  $V_o$ . Similarly, if the rms voltage  $V_s$  exceeds the reference voltage, the ES will suppress it to the reference value  $V_{s-ref}$ , by allowing non-critical load voltage to vary dynamically. In other words, ES will manipulate the

current  $I_0$  and in turn  $I_{in}$  in the circuit of Fig 2 such that Equation (4) is satisfied,

$$V_{in} - I_{in}(R_x + j\omega L_x) = V_s = V_{s\_ref} \quad (4)$$

### B. ES and other FACTS Devices: A Comparative Analysis

ES has recently been proposed as a novel and simple way of distributed voltage control while simultaneously enabling effective demand-side management without any need for communication [15]. Unlike ES, the existing FACTS devices have a centralized approach, which must be implemented throughout the grid.

The ES injects a series voltage in quadrature (either lead or lag) with the current flowing through the non-critical loads to regulate the voltage across the point of common coupling where critical (i.e., voltage-sensitive) loads are connected. The approach fundamentally differs from the traditional way of shunt voltage control through SVC, STATCOM, etc., which are connected at the point-of-common-coupling (PCC) to control the voltage across several loads [16].

The electric spring differentiates itself from a traditional Reactive Power Compensator (RPC) by adopting an “input-voltage control.” By regulating the input voltage and letting the output voltage fluctuate dynamically (i.e., a new input-voltage control), an ES would 1) provide voltage support and 2) simultaneously modulate the non-critical load power to follow the power generated. Such a subtle change in the control strategy of a traditional RPC from output control to input control offers a new possibility of simultaneous voltage and frequency control, enabling effective demand side management.

### C. Modeling of ES as a Reactive Power Compensator

The reactive power exchange with the ES depends on the injected voltage  $V_{ES}$  and also on the impedance of the NC load. Consider the circuit shown in Fig. 3 [7].

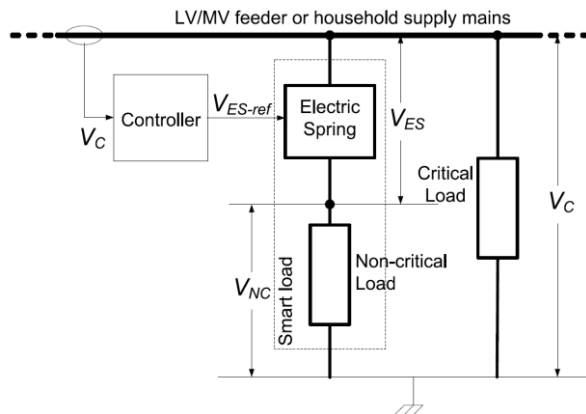


Fig. 3. Electric spring set up for smart loads [7].

For a resistive-inductive type NC load with impedance  $Z_{NC}$ , the voltages  $V_C$ ,  $V_{ES}$  and  $V_{NC}$  are shown in the phasor diagram in Fig. 4. In case the ES is working in voltage support (i.e., capacitive) mode, as shown by the phasor diagram,

$$V_C^2 = (V_{NC} - V_{ES}\sin\theta_{NC})^2 + (V_{NC} - V_{ES}\cos\theta_{NC})^2 \quad (5)$$

$$V_{NC} = \pm\sqrt{(V_C^2 - (V_{ES}\cos\theta_{NC})^2) + V_{ES}\sin\theta_{NC}} \quad (6)$$

$$Q_{ES} = V_{ES}I_{NC}\sin(-90^\circ) = -V_{ES}I_{NC} = -\frac{V_{ES}V_{NC}}{Z_{NC}} \quad (7)$$

$$Q_{NC} = V_{NC}I_{NC}\sin(\theta_{NC}) = \frac{V_{NC}^2}{Z_{NC}}\sin(\theta_{NC}) \quad (8)$$

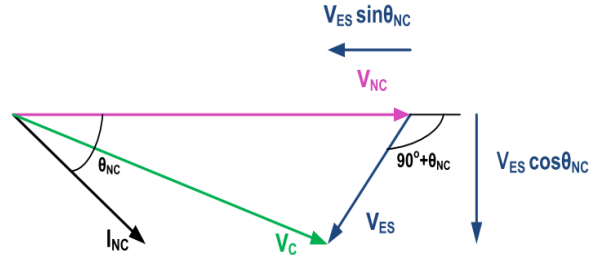


Fig. 4. Phasor relationships between voltages across non-critical load, critical load, and ES.

Here,  $Q_{ES}$  and  $Q_{NC}$  are the reactive powers of the ES and the NC load, respectively. For a purely resistive NC load, the reactive power of the ES and the smart load will be equal. However, they would be different if the NC is not purely resistive. If the ES is working in voltage support (i.e., capacitive) mode with an NC load of R-L type, the total reactive power of the smart load  $Q_{SL}$  is given by,

$$\begin{aligned} Q_{SL} &= Q_{ES} + Q_{NC} = \\ &= \frac{-V_{ES}(\pm\sqrt{V_C^2 - V_{ES}\cos\theta_{NC}^2} + V_{ES}\sin\theta_{NC})}{Z_{NC}} \\ &\quad + \frac{(\pm\sqrt{V_C^2 - V_{ES}\cos\theta_{NC}^2} + V_{ES}\sin\theta_{NC})}{Z_{NC}}\sin\theta_{NC} \end{aligned} \quad (9)$$

Similarly, for the ES in voltage suppress (i.e., inductive) mode,

$$\begin{aligned} Q_{SL} &= \frac{V_{ES}(\pm\sqrt{V_C^2 - V_{ES}\cos\theta_{NC}^2} - V_{ES}\sin\theta_{NC})}{Z_{NC}} \\ &\quad + \frac{(\pm\sqrt{V_C^2 - V_{ES}\cos\theta_{NC}^2} - V_{ES}\sin\theta_{NC})}{Z_{NC}}\sin\theta_{NC} \end{aligned} \quad (10)$$

From Equations (7), (9), and (10), it is clear that the reactive power of the ES and the smart load are both dependent on NC load impedance.

#### D. Distribution Load Flow Algorithm

In this work, a direct approach to the distribution load flow method [17] is used to satisfy all the technical constraints of the network. The two matrices, developed from the topological characteristics of distribution systems, are used to solve the load flow problem. The bus-injection to branch-current (BIBC) matrix represents the relationship between bus current injections and branch currents, and the branch-current to bus-voltage (BCBV) matrix represents the relationship between branch currents and bus voltages. The corresponding variations in bus voltages, generated by the variations at branch currents, can be calculated directly by the BCBV matrix; these two matrices are combined to form a direct approach for solving load flow problems [17]. The relationship between bus current injections and bus voltages can be expressed as:

$$\Delta V = [BCBV][BIBC][I] - [DLF][I] \quad (19)$$

where, DLF refers to the Distribution Load Flow matrix. The solution for distribution load flow can be obtained by solving Equation (19) iteratively.

For bus, the complex load  $S_i$  is expressed by,

$$S_i = P_i + Q_i \quad i = 1, \dots, N \quad (20)$$

And the corresponding equivalent current injection at the  $k^{th}$  iteration of the solution is,

$$I_i^k = I_i^r(V_i^k) + jI_i^k(V_i^k) = (\frac{P_i + Q_i}{V_i^k})^* \quad (21)$$

where,  $V_i^k$  and  $I_i^k$  are the bus voltage and equivalent current injection of bus  $i$  at the  $k^{th}$  iteration, respectively. The current  $I_i^r$  and  $I_i^i$  are the real and imaginary parts of the equivalent current injection of bus  $i$  at the  $k^{th}$  iteration, respectively.

### 3. SUGGESTED METHODOLOGY

### A. Suggested Formulation of ES: A Power Injection Model

This work suggests a power injection model of ES as follows. The power circuit of the Electric Spring and that of the Smart Load, including the Electric Spring, are taken from ref. [15] as shown in Figs. 5 and 6, respectively.  $V_{ES}$  represents the voltage injected by the Electric Spring and  $I_f$ ,  $R_f$  and  $C_f$  are the inductance, resistance and capacitance of the output filter at the inverter terminal. These three compose the overall filter impedance  $Z_f$ . All the impedances, voltages and currents are phasors.

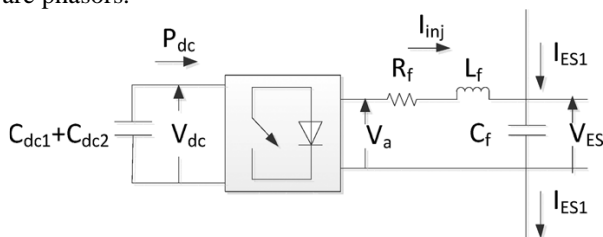


**Fig. 5. Power circuit of electric spring [15].**

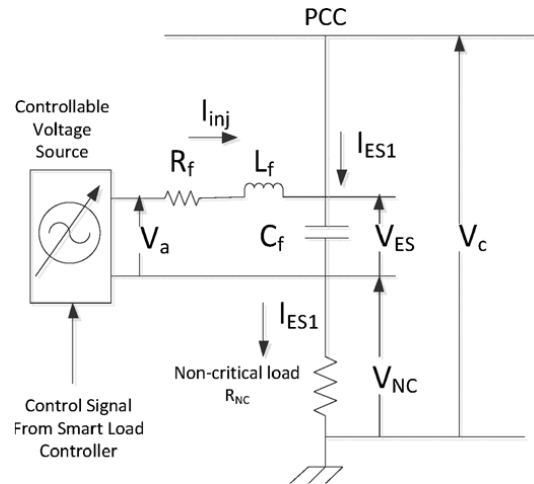


**Fig. 6. Model for the power circuit of smart load and electric spring [15].**

The Power Injection Model is derived using a series of KVL and KCL Equations from the power circuit of the ES, as shown in Fig. 5. Applying KVL on the AC side of the inverter:

$$I_{inj} = \frac{V_a - V_{ES}}{Z_f} \quad (11)$$

where,  $I_{inj}$  is the output of the inverter and  $V_a$  is the terminal voltage of the half-bridge inverter.

Applying KVL between PCC and the reference ground,

$$I_{ES1} = \frac{V_C - V_{ES}}{Z_{NC}} \quad (12)$$

The injection current  $I_{inj}$  flows in a loop through the filter circuit and the inverter. While the current  $I_{ES1}$  flows from PCC to the ground through the filter capacitor and the non-critical load, as shown in Fig. 6.

The voltage across the filter capacitor can be expressed as:

$$\begin{aligned} V_{ES} &= X_C (I_{ES1} + I_{inj}) = j\omega C * V_{ES} \\ &= I_{ES1} + I_{inj} \end{aligned} \quad (13)$$

Substituting Equations (11) and (12) in Equation (13),  $j\omega C * V_{ES} = \frac{V_a - V_{ES}}{Z_f} + \frac{V_C - V_{ES}}{Z_{NC}} = -V_{ES} \left( \frac{1}{Z_f} + \frac{1}{Z_{NC}} \right) + \frac{V_a}{Z_f} + \frac{V_C}{Z_{NC}}$  or

$$V_{ES} = \frac{\frac{V_a}{Z_f} + \frac{V_C}{Z_{NC}}}{j\omega C + \frac{1}{Z_{NC}} + \frac{1}{Z_f}} \quad (14)$$

The average output voltage  $V_a$  of the half-bridge inverter is given by Equation (15) as follows,

$$V_a = m * V_{DC}/2 \quad (15)$$

where,  $V_{DC}$  is the DC link voltage and  $m$  is the modulation index of the inverter.

Substituting Equations (14) and (15) in Equation (12),

$$I_{ES1} = \frac{V_C}{Z_{NC}} - \frac{\frac{V_a}{Z_f} + \frac{V_C}{Z_{NC}}}{Z_{NC}(j\omega C + \frac{1}{Z_{NC}} + \frac{1}{Z_f})} \quad (16)$$

$$= \frac{V_C}{Z_{NC}} - \frac{\frac{m * V_{DC}/2}{Z_f} + \frac{V_C}{Z_{NC}}}{Z_{NC}(j\omega C + \frac{1}{Z_{NC}} + \frac{1}{Z_f})}$$

Thus, the total power injected by the Smart Load (ES connected in series with the NC load) is given by:

$$S_{after} = V_C * I_{ES1}$$

$$= V_C * (\frac{V_C}{Z_{NC}} - \frac{\frac{m * V_{DC}/2}{Z_f} + \frac{V_C}{Z_{NC}}}{Z_{NC}(j\omega C + \frac{1}{Z_{NC}} + \frac{1}{Z_f})}) \quad (17)$$

However, the power consumed by the NC load without the ES is given by,

$$S_{before} = V_C * I_{ES1} = V_C * (\frac{V_C}{Z_{NC}}) \quad (18)$$

### B. Proposed Placement of ES in Distribution Systems

This work proposes an optimal placement of ES for voltage improvement based on the existing Voltage Stability Index (VSI) method suggested in ref. [18]. It is an index to determine the static voltage stability of the load buses in a power network for certain operating conditions. Hence, it identifies load buses that are close to voltage collapse. This index is formulated from the quadratic equation derived from a two-bus network and is computed using the apparent power and the line impedance. The values of VSI show how far the load buses are from their voltage stability limit; hence, the most sensitive bus can be identified according to maximum loadability. Transferred active and reactive power expressions of the distribution line are used for developing the stability index and only require a power flow solution of the system at any operating condition. Other details are skipped in this work for the sake of space, which is available in ref. [18].

## 4. RESULTS AND DISCUSSION

### A. The Developed Power Injection Model of ES

The values of the various physical parameters considered for the calculation of ES effects are as follows:

$V_C$  : 230 volts as the reference voltage and 240 volts as the fluctuated voltage.

Phase = Zero degrees

$V_{DC}$  : 400 volts

$Z_{NC}$  :  $R_{NC} = 6.11$  Ohms;  $L_{NC} = 1.893 \times 10^{-3}$  Henry

$Z_C$  :  $R_C = 11$  Ohms;  $L_C = 3.9 \times 10^{-3}$  Henry

$Z_f$  :  $R_f = 3$  Ohms;  $L_f = 1.92 \times 10^{-3}$  Henry;  $C = 13.2 \times 10^{-6}$  Farad  
 $m=1$

The frequency that has been used for this calculation is 50 Hz.

Substituting these values in the developed formula, i.e., Equation (18) for the power consumed by the non-critical load before ES was connected as follows.

$$Q_{before} = -2.8 \text{ VAR}$$

Substituting the required values in the developed formula, i.e., Equation (17) for the power supplied by the Smart Load (non-critical load and ES) as,

$$Q_{after} = -1178 \text{ VAR}$$

Hence, the reactive power consumed by ES to bring down the voltage from 240 V to 230 V is,

$$Q_{after} - Q_{before} = -1178 + 2.8 = -1175.2 \text{ VAR}$$

This reactive power value shows that ES has to transfer from critical to non-critical load to bring a fluctuated voltage of 240 V to 230 V as reference one.

### B. Studying the Effect of ES on a 3-bus System

This section considers the developed power injection model of ES (given in section 3-A) as follows. A standard 3-bus distribution network has been chosen for the load flow analysis. The system is designed and studied using PSAT software [19], as shown in Fig. 7. Without any compensation as Base case, DSTATCOM as Case-1 and ES as Case-2 are considered here to understand the effect of the ES in the system. In all three cases, the base voltage is considered to be 220 V at 10 kVA base.

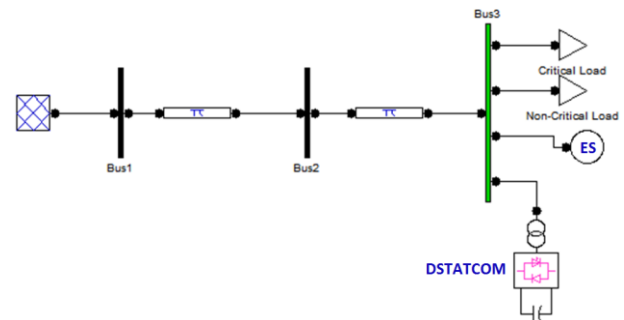


Fig. 7. Standard 3-bus System with both ES and DSTATCOM in PSAT.

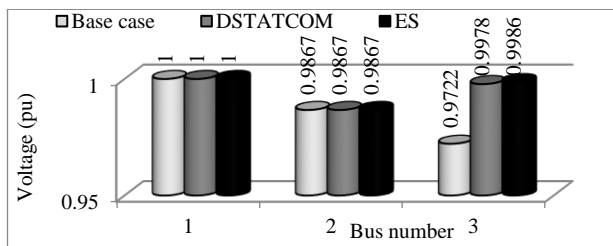
#### 1) Base Case: without any compensators

To study this case, the 3-bus system is simulated without any of the reactive power compensators, i.e., ES as well as DSTATCOM are both disabled in the circuit diagram shown in Fig. 7. The system parameters chosen are mentioned in Table 1. Load flow analysis was carried out on this 3-bus system and the corresponding voltage, real power and reactive power were measured at each of the buses.

**Table 1. System parameters for the 3-bus system.**

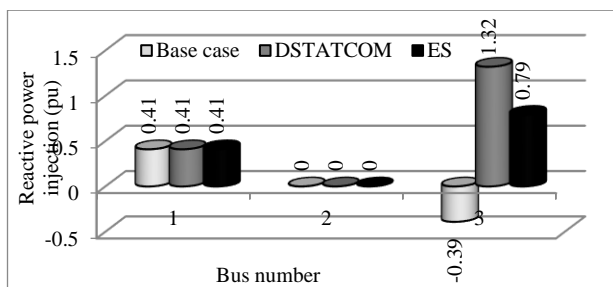
Description	Value(ohms)
Line Impedance	$0.1+0.0024i$
Critical Load	$11+0.0039i$
Non-critical Load	$6.11+0.0019i$

Figure 8 and Table 2 show the results for all three cases. Figure 8 shows a gradual drop in the voltages from bus-1 to 3, as shown by light-colored bars in Fig. 8. This drop can be attributed to the drops in the transmission line. Similarly, from Fig. 9, the reactive power injections and absorptions are shown at each bus. The difference in reactive power injections between buses-1 and 3 is due to the line losses.

**Fig. 8. Bus voltage profile in all three cases.**

### 2) Case-2: with DSTATCOM

In this case, only DSTATCOM is enabled at bus-3, as observed in Fig. 7. The DSTATCOM has a rating of 10 kVA, 220 volts. From the medium black colored bars in Figure 8, it could be observed that there is a considerable increase in the voltage magnitude at bus-3, where the DSTATCOM is connected. It rose from 0.9722 to 0.9978 pu as compared to the Base case. Here, DSTATCOM is connected to bus-3, which injects reactive power and that's why the voltage level is now maintained close to the reference value of 1.0 pu at bus-3. From medium black colored bars in Fig. 9, it can be seen that there is an injection of 1.32 pu of reactive power at bus-3 compared to an absorption of 0.39 pu as in the Base case.

**Fig. 9. Reactive power injections in all three cases.**

### 3) Case-2: with Electric Spring

This case analyses the effect of placing an ES by only enabling it at bus-3. The ES is considered to be lossless. It just acts as a source or sink of reactive power that leads to control of node voltage where it is placed. From Equation (17), the amount of power injected into the bus

is calculated and added to the non-critical load as they are connected in series. The various parameters of ES used to calculate the load flow results are considered the same as those in section 4-A, except  $V_C$  is taken here as 220 V instead of 230 V.

After load flow analysis, it can be observed from light-colored bars in Fig. 8 that the voltage at bus-3 was boosted up to 0.9986 pu from base case voltage 0.9722 pu. Regarding reactive power flow, the ES, in conjunction with the non-critical load, acts as a Smart Load. Similarly, from the dark black bars in Fig. 9, it could be observed that the amount of reactive power was injected or absorbed in 3 buses from ES. It can be seen that the net reactive power at bus-3 is positive.

**Table 2. Comparison of parameters for the 3-bus system.**

Description	Base Case	DSTATCOM	ES
Voltage at bus-3 (pu)	0.9722	0.9978	0.9986
Reactive power at bus-3 (pu)	-0.39	1.32	0.79
% Voltage Regulation at bus-3	-	22	14

From the load flow analysis of the 3-bus system, it can be concluded that the ES gives a better voltage regulation by 8 percent than a DSTATCOM. Moreover, the reactive power capacity of the ES required to achieve this much is less than that of DSTATCOM.

## C. A Comprehensive Study of a 14-bus Network with ES

This study involves a more comprehensive analysis of how the placement of an ES affects the system and also compares performances with DSTATCOM. Here, a complex, standard network consisting of 14 buses is chosen from the PSAT library. The network already consists of a DSTATCOM rated at 1.1 kV and 100 kVA on the 14<sup>th</sup> bus as shown in Fig. 10.

### 1) Base Case: without any compensators

To study the base case, both ES and DSTATCOM are disabled in the circuit diagram of Fig. 10. The voltage profile is seen in Fig. 11. The presence of synchronous compensators at bus-3 and 6 is the reason for which reactive power is injected into the network at those buses.

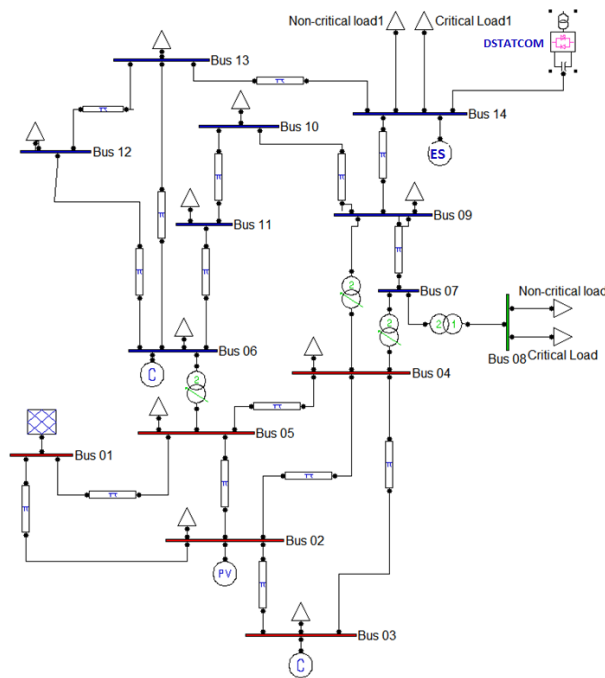


Fig. 10. Standard 14-bus system from PSAT [19].

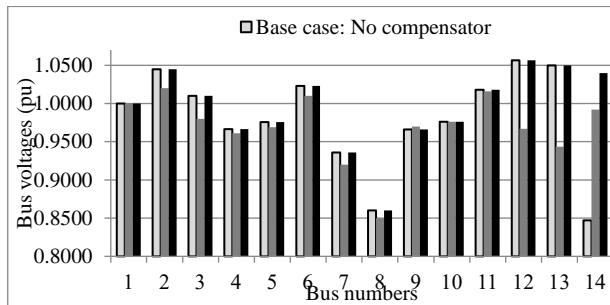


Fig. 11 Voltage profile in different cases

### 2) Case-1: with DSTATCOM

In this case, a DSTATCOM is being inserted into the network at the 14<sup>th</sup> bus and its effects are studied. The light-dark bars in Fig. 11 show the voltage profile when the DSTATCOM is operating. The voltage at bus-14 is

boosted up to 0.992 pu, which is close to the reference value set to 1.04 pu in this case. The DSTATCOM is a reactive power source, and it feeds reactive power into the network so that the voltage can be boosted up at the 14<sup>th</sup> bus. In this case, it supplies a reactive power of 1.19 pu into the bus-14.

### 3) Case-1: with Electric Spring

Finally, the DSTATCOM is replaced with an ES to compare their working and effects on the network. The load on bus-14 has been separated into critical and non-critical loads in the ratio 1:1, as shown in Fig. 10. The ES is considered to be lossless, and no active power is injected or absorbed by it. It just acts as a source or sink of reactive power that leads to control of node voltage. From Equation (17), the amount of power injected into the bus is calculated and added to the non-critical load as they are connected in series. The ES, in conjunction with the non-critical load, forms the smart load that is responsible for maintaining the voltage at the reference value of the candidate bus. In Figure 11, the ES maintains a voltage higher than the previous case and nearly equal to the reference value of 1.04 pu, as black bars show. However, the reactive power injected into the 14<sup>th</sup> bus by the ES is about 9% lower than the amount injected by the DSTATCOM.

### D. Optimal Placement of the ES in 33-bus to Improve the Voltage Profile

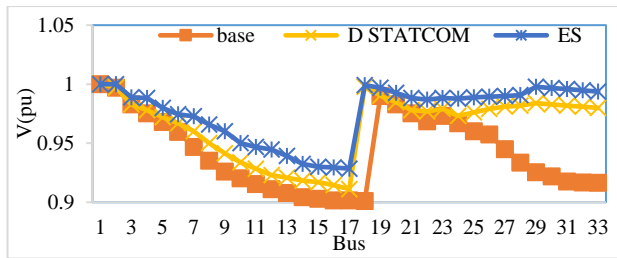
The ES, being used as a reactive power compensator, needs to be placed optimally in the distribution system. For this purpose, an IEEE 33-bus radial distribution network [20] is chosen and its stability analysis is carried out. The Voltage Stability Index is calculated [18] for each node to identify the most unstable bus and only 20 values in descending order are shown in Table 3. This table depicts the voltage stability index for each bus. It could be noted that bus-30 has the highest index and is closest to 1. Hence, it is the candidate bus for placing the ES as it is the most unstable one.

Table 3. VSI for 33-bus system.

Order no.	BN	VSI	Order no.	BN	VSI	Order no.	BN	VSI	Order no.	BN	VSI
1	30	0.0296	6	20	0.0041	11	18	0.0024	16	22	0.0019
2	25	0.0122	7	29	0.0037	12	32	0.0024	17	4	0.0016
3	24	0.0120	8	13	0.0035	13	9	0.0020	18	6	0.0015
4	8	0.0119	9	14	0.0028	14	10	0.0020	19	16	0.0015
5	31	0.0052	10	17	0.0026	15	28	0.0020	20	3	0.0013

In this work, three cases are considered like base cases: without any compensators, case-2, with DSTATCOM placed on the candidate bus, and case-3, with an ES placed on the same bus. Further, the load flow technique being used is described in section 2-D. Various physical parameters were studied and compared,

including active and reactive power flows and voltages. Figure 12 shows the voltage profile for each of the cases.



**Fig. 12 Voltage profile for 33 bus system**

The various graphs in Fig. 12 show the effectiveness of ES over DSTATCOM. The voltage that is measured in per unit keeps on decreasing till bus-18, which was found to be the lowest voltage in all the 3 cases. Owing to the configuration of the network it increases from 19<sup>th</sup> bus onwards and, only to decrease again as move further away from the source. It could be noticed that the voltage profile of the third case (with ES) lies above the rest two cases, and the voltage at the candidate bus is boosted near to unity. The DSTATCOM also enhances the voltage as compared to the base case but still lags the ES. The underlying Table 4 gives a detailed description and comparison of the various parameters.

Analyzing the results given in Table 4, it could be noted that the number of buses with lower voltages is

reduced from 21 to 10 when a DSTATCOM or an ES is connected. The minimum voltage is recorded at the 18<sup>th</sup> bus in each case. An interesting thing to be observed is that the candidate bus is not on the 18<sup>th</sup> but on the 30<sup>th</sup> bus. This can be due to the fact that the stability index of the 30<sup>th</sup> is closest to 1 and is the most unstable.

On comparing the effect of both ES and DSTATCOM on the voltage, as shown in Table 4, it is observed that the ES regulates the voltage better than the DSTATCOM at the 18<sup>th</sup> bus. At the same time, the amount of reactive power needed to achieve the voltage boost is less in an ES than in the DSTATCOM.

#### **E. Optimal placement of the ES in the 69-bus system**

Further, a somewhat bigger system, i.e., a 69-bus radial distribution network [21], has been chosen. Inspection to find out the most unstable bus is carried out using the same voltage stability index. The first 20 voltage stability indices are only shown in Table 5 for the sake of space.

It could be noticed that the 61<sup>st</sup> bus is the most unstable one with the highest voltage stability index. The results for the similar three cases with and without an ES/DSTATCOM are compared as shown in Fig. 15.

**Table 4. Comparison of Parameters for 33-bus system.**

Description	Base Case	With DSTATCOM	With ES
Total Active Power Load in kW	3715	3715	3715
Total Reactive Power Load in kVAr	2300	2300	2300
No of Buses with voltage deviations	21	10	10
Optimal Location	-	30 <sup>th</sup> Bus	30 <sup>th</sup> Bus
Reactive Power Injected (MVar)	-	1.9930	1.5450
Minimum voltage (pu) (18 <sup>th</sup> bus)	0.9015	0.9111	0.9285

**Table 5. VSI for 69-bus system.**

Order no.	BN	VSI	Order no.	BN	VSI	Order no.	BN	VSI	Order no.	BN	VSI
1	61	0.2952	6	64	0.2119	11	26	0.1634	16	21	0.1612
2	60	0.2789	7	63	0.2086	12	25	0.163	17	20	0.1597
3	59	0.2635	8	62	0.2076	13	24	0.1624	18	19	0.1584
4	58	0.2416	9	57	0.1911	14	23	0.162	19	18	0.1574
5	65	0.2158	10	27	0.1635	15	22	0.1618	20	17	0.1563

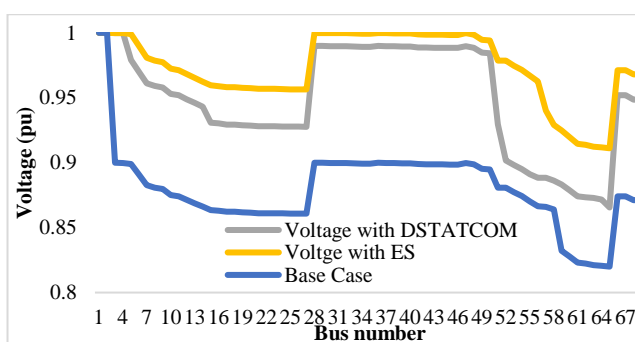


**Fig. 13. Voltage profile for 69 bus system.**

Figure 13 indicates how the ES, when placed at the candidate bus, boosts up the voltage to near unity. The overall voltage profile of the network is also improved. Further, Table 6 shows the comparative results with and without the ES/DSTATCOM effects on the network. It could be seen that the minimum voltage at the 65<sup>th</sup> bus is boosted up to 0.9111 pu from 0.8199 when an ES is placed at the 61<sup>st</sup> bus, which is the candidate bus.

**Table 6. Comparison of parameters for 69 bus system**

Description	Base Case	With DSTATCOM	With ES
Total Active Power Load in kW	3790	3790	3790
Total Reactive Load in kVAr	2700	2700	2700
Min voltage (pu) (65 <sup>th</sup> bus)	0.8199	0.8655	0.9111
Optimal Location	-	61 <sup>st</sup> bus	61 <sup>st</sup> bus

## 5. CONCLUSION

This paper suggests a step-by-step approach from developing a power injection model to analyze the ES's electric voltage boosting property. Initially, a generalized Power Injection Model is formulated for the ES, which is applied and tested using the simulation results. Finally, the developed power injection model optimizes the ES in the distribution network based on the voltage stability index. Based on the results of this paper, the ES has great potential to replace the conventional reactive power compensators, provided that deviations are in the scope of ES. Further, it can act as a smart load in conjunction with the existing dissipating loads in the grid, which can surely be a part of the future of smart and sustainable grids.

Further studies can be carried out to integrate it with energy storage and damping electric oscillations applications of the Electric Spring.

## REFERENCES

- [1] Eltawil, M. A., & Zhao, Z. (2010). Grid-connected photovoltaic power systems: Technical and potential problems—A review. *Renewable and Sustainable Energy Reviews*, 14(1), 112–129.
- [2] Katiraei, B. F. (2011). Studies for Utility-Scale Photovoltaic Distributed Generation. *Ieee Power And Energy Magazine*, 9(3), 62–71.
- [3] Dixon, J., Moran, L., Rodriguez, J., & Domke, R. (2005). Reactive Power Compensation Technologies: State-of-the-Art Review. *Proceedings of the IEEE*, 93(12), 2144–2164.
- [4] Kundur, P., Balu, N. J., & Lauby, M. G. (1994). Power system stability and control.
- [5] Lee, C. K., Li, S., & Hui, S. Y. (2011). A design methodology for smart LED lighting systems powered by weakly regulated renewable power grids. *IEEE Transactions on Smart Grid*, 2(3), 548–554.
- [6] Hui, S. Y., Lee, C. K., & Wu, F. F. (2012). Electric Springs; A New Smart Grid Technology. *IEEE Transactions on Smart Grid*, 3(3), 1552–1561.
- [7] Xiao, L., S., Akhtar, Z., & Lee, C. K. (2015). Distributed Voltage Control with Electric Springs: Comparison with STATCOM, *IEEE Transactions on Smart Grid*, 6(1), 209–219.
- [8] Muhammad S. Javaid, Adeel Sabir, M.A. Abido, H.R.E.H. Boucekara. “Design and implementation of electric spring for constant power applications,” *Electric Power Systems Research*, Volume 175, October 2019, 105884.
- [9] Cui, Zhibin, Junsheng Shi, Guangpeng Li, Zihan Yuan, Dehua Zang, and Lidi Wang. 2023. "The Application of Photovoltaic-Electric Spring Technology to Rural Power Grids" *Processes* 11, no. 6: 1830. <https://doi.org/10.3390/pr11061830>.
- [10] Lee, C. K., Tan, S. C., Wu, F. F., Hui, S. Y. R., & Chaudhuri, B. (2013). Use of Hooke's law for stabilizing future smart grid the electric spring concept. *2013 IEEE Energy Conversion Congress and Exposition, ECCE 2013*, (1), 5253–5257.
- [11] J. Zhang, Y. Wu, M. Liu and W. Ji, "Research on Application of DC Electric Spring in DC Distribution Network," *The 10th Renewable Power Generation Conference (RPG 2021)*, Online Conference, 2021, pp. 338-343, doi: 10.1049/icp.2021.2290.
- [12] Guillermo Tapia-Tinoco, David Granados-Lieberman, Martin Valtierra-Rodriguez, Juan Gabriel Avina-Cervantes, Arturo Garcia-Perez, “Modeling of electric springs and their multi-objective voltage control based on continuous genetic algorithm for unbalanced distribution networks,” *International Journal of Electrical Power & Energy Systems*, Volume 138, 2022, 107979, ISSN 0142-0615, <https://doi.org/10.1016/j.ijepes.2022.107979>.
- [13] Wahl, A. M. (1944). *Mechanical Springs Arthur, M. M., & Co, P. P.*
- [14] Jayantika Soni, Krishnanand K R, and S K Panda, “Load-side Demand Management in Buildings using Controlled Electric Springs”, Industrial Electronics Society, IECON 2014 - 40th Annual Conference of the IEEE, pp. 2014. DOI: 10.1109/IECON.2014.7049321
- [15] Chaudhuri, N. R., Lee, C. K., Chaudhuri, B., & Hui, S. Y. R. (2014). Dynamic Modeling of Electric Springs, *IEEE Transactions on Smart Grid*, Vol. 5, No. 5, pp. 2450 – 2458, September 2014.
- [16] Hingorani, N.G. and Gyugyi, L. (1999), *Understanding FACTS Concepts and Technology of Flexible AC Transmission Systems*. Wiley-IEEE Press, New York.
- [17] Teng, J.-H. (2003). A direct approach for distribution system load flow solutions. *IEEE Transactions on Power Delivery*, 18(3), 882 – 887.
- [18] Jalboub M. K., H. S. Rajamani, D. T. W. Liang, R. A. Abd-Alhameed & A. M. Ithal (2010). Investigation of Voltage Stability Indices to Identify Weakest Bus (TBC), *6th International ICST Conference, MOBIMEDIA*.
- [19] Power System Analysis Toolbox, <http://faraday1.ucd.ie/index.html>.
- [20] M. E. Baran and F. Wu, “Network reconfiguration in distribution system for loss reduction and load

- balancing,” *IEEE Trans. Power Del.*, vol. 4, no. 2, pp. 1401–1407, Apr. 1989.
- [21] M. E. Baran and F. Wu, “Optimal capacitor placement on radial distribution systems,” *IEEE Trans. Power Del.*, vol. 4, no. 1, pp. 725–734, Jan. 1989.